Chinese Journal of Catalysis 36 (2015) 1358–1364

available at www.sciencedirect.com

ScienceDirect

journal homepage: www.elsevier.com/locate/chnjc

Article

Bimetallic synergistic Au/CuO-hydroxyapatite catalyst for aerobic oxidation of alcohols

Tao Tian, Ying Liu, Xungao Zhang *

College of Chemistry and Molecular Sciences, Wuhan University, Wuhan 430072, Hubei, China

ARTICLE INFO

Article history:
Received 10 February 2015
Accepted 27 March 2015
Published 20 August 2015

Keywords:
Heterogeneous catalysis
Gold-copper bimetallic catalyst
Aerobic oxidation of alcohols
Hydroxyapatite
Reusability

ABSTRACT

A catalyst consisting of Au supported on copper oxide-modified hydroxyapatite (Au/CuO-HAP) was prepared using a homogeneous deposition-precipitation method. The catalyst was characterized using atomic absorption spectrometry, N_2 adsorption-desorption, powder X-ray diffraction, transmission electron microscopy, and X-ray photoelectron spectroscopy. The catalytic performance in liquid-phase aerobic oxidation of alcohols was investigated. The catalytic activity and benzaldehyde selectivity in benzyl alcohol oxidation with the bimetallic Au/CuO-HAP catalyst were significantly better than those with monometallic Au/HAP and CuO-HAP catalysts. The conversion of benzyl alcohol and selectivity for benzaldehyde at 120 °C for 1.5 h under aerobic oxidation conditions were 99.7% and 98.4%, respectively. Various aromatic alcohols were selectively converted to their corresponding aldehydes or ketones over Au/CuO-HAP. The Au/CuO-HAP catalyst could be reused at least four times without loss of activity.

1. Introduction

Liquid-phase oxidation of alcohols to the corresponding ketones or aldehydes is important in organic functional group conversion reactions [1]. Traditionally, stoichiometric oxidants such as dichromate and permanganate have been used in the oxidation of alcohols [2–5]. However, excessive use of these stoichiometric oxidants raises environmental and safety concerns. In addition, many by-products are generated because of over oxidation. In terms of cost saving and environmental protection, new routes to aldehydes and ketones using benign oxidizing agents such as organic peroxides, hydrogen peroxide, and molecular oxygen are of significant interest [6–8]. Nanomaterials based on noble metals such as Pd, Au, Pt, and Ru have been widely studied as potential catalysts [9–12].

Au was considered to be an inert material until Haruta et al. [13,14] showed that well-dispersed Au nanoparticles (NPs, below 10 nm) supported on TiO_2 show high activity in the low-temperature CO oxidation. In the last two decades, nanosized Au catalysts have attracted much attention because of their high catalytic activity in various reactions [15,16]. Recently, bimetallic Au catalysts have been found to have better catalytic activity and selectivity than monometallic catalysts, because of their tunable and synergistic properties; for example, Au-Pd/TiO_2 catalysts have been used in the oxidation of primary carbon-hydrogen bonds in toluene [17], oxidation of primary alcohols [18], cinnamaldehyde hydrogenation [19], and direct hydrogen peroxide synthesis [20]. Zhao et al. [21] reported that the stability and catalytic lifetime of a Au/γ-Al_2O_3 catalyst could be improved by the addition of Bi. Zhang et al. [22] found that Au in cooperation with Co gave superior catalytic activity and long-term stability in acetylene hydrochlorination.

Supported bimetallic Au-Cu catalysts have been widely used

* Corresponding author. Tel/Fax: +86-27-68752136; E-mail: xgzhang66@whu.edu.cn
This work was supported by Natural Science Foundation of Hebei Province of China (2013CFB291).
DOI: 10.1016/S1872-2067(15)60854-3 | http://www.sciencedirect.com/science/journal/18722067 | Chin. J. Catal., Vol. 36, No. 8, August 2015

in CO preferential oxidation [23], CO_2 reduction [24], hydrogenation of cinnamaldehyde [25], and gas-phase oxidation of benzyl alcohol [26]. Recently, Li et al. [27] reported that silica-supported Au-Cu alloy NPs showed good activity and selectivity for aldehydes in liquid-phase oxidation of alcohols under mild and base-free conditions, but rigorous post-processing such as reduction with H_2 at 550 °C was necessary for catalyst recovery. A CuO-supported Au catalyst with high selectivity and activity for benzyl alcohol oxidation under mild conditions has been reported [28]. In this study, we prepared and characterized Au supported on CuO-modified hydroxyapatite (Au/CuO-HAP), and investigated its catalytic properties in the oxidation of alcohols. The Au/CuO-HAP performance was better than those of monometallic Au/HAP and CuO-HAP, and it had excellent recyclability. Various aromatic alcohols were efficiently converted to their corresponding aldehydes or ketones over Au/CuO-HAP under aerobic conditions.

2. Experimental

All reagents were analytical grade and purchased from the Sinopharm Chemical Reagent Co., Ltd. They were used without further purification unless otherwise specified. Deionized water was used in all experiments.

2.1. Preparation of HAP and CuO-HAP supports

HAP was prepared as follows. Phosphoric acid aqueous solution (300 mL, 0.1 mol/L) was added dropwise to an aqueous suspension (300 mL) of calcium hydroxide (3.71 g, 0.05 mol) under vigorous mechanical stirring. The dropping speed was controlled at 4 mL/min, the temperature of the suspension solution was set at 80 °C, and the pH of the suspension solution was adjusted to 9.0 with aqueous ammonia. After addition of the phosphoric acid solution, the mixture was stirred at 80 °C for 3 h. The resulting precipitate was collected by filtration and washed with deionized water. The solid was dried at 105 °C overnight, and then calcined at 500 °C for 3 h.

The CuO-HAP support was prepared by dropwise addition of an aqueous solution (300 mL) of phosphoric acid (3.68 g, purity 85%) and copper(II) chloride dihydrate (0.571 g) to an aqueous suspension (300 mL) of calcium hydroxide (3.71 g), with vigorous mechanical stirring; the molar ratio of (Ca + Cu)/P was set at 1.67. The subsequent procedures were the same as those for HAP preparation. The resulting product was denoted by CuO-HAP.

2.2. Preparation of Au/HAP and Au/CuO-HAP catalysts

The Au/HAP and Au/CuO-HAP catalysts were prepared using the homogeneous deposition-precipitation method developed by Zanella et al. [29], using urea as the precipitating agent. HAP or CuO-HAP (0.5 g) was added to an aqueous solution (20 mL) of $HAuCl_4{\cdot}4H_2O$ (5.3×10^{-3} mol/L) and urea (0.84 mol/L). The suspension was heated to 90 °C and stirred for 4 h. The solid was separated by centrifugation and washed with deionized water until no chloride ions were detected (using $AgNO_3$ solution) in the supernatant. The solid was dried at 90 °C overnight and calcined at 300 °C for 4 h in air flow (30 mL/min). The obtained purple catalysts were denoted by Au/HAP and Au/CuO-HAP.

2.3. Catalyst characterization

The Au and Cu contents of the catalysts were determined using atomic absorption spectrometry (AAS; Perkin-Elmer PEAA800). The specific surface areas of the catalysts were determined from their N_2 adsorption-desorption isotherms at −196 °C by the Brunauer-Emmett-Teller method, using a Tristar II 3020 V1.02 instrument (Micromeritics Instrument Corporation, USA). The pore size distributions were obtained from the desorption branch of the N_2 adsorption-desorption isotherms using the Barrett-Joyner-Halenda (BJH) method. The crystal structure of the catalysts were examined using powder X-ray diffraction (XRD; X'Pert Pro, PANalytical, Cu K_α radiation (λ = 0.15406 nm), operated at 40 mA and 40 kV). Transmission electron microscopy (TEM) and high-resolution TEM (HRTEM) were performed using a JEOL JEM-2010-HR microscope operated at 200 kV. Before the TEM experiments, the samples were ultrasonically dispersed in ethanol and transferred to a Cu grid coated with a holey carbon film. The chemical states of the surface elements were determined using X-ray photoelectron spectroscopy (XPS; ESCALAB 250Xi, Thermo Fisher) with monochromic Al K_α radiation; all binding energies were calibrated using the C 1*s* line at 284.8 eV.

2.4. Catalytic reaction

The alcohol aerobic oxidations were performed in a bath-type reactor under oxygen (101.3 kPa). In a typical reaction, a 25 mL three-necked round-bottomed flask containing alcohol (3 mmol), K_2CO_3 (1 mmol), a certain amount of catalyst, and *p*-xylene (10 mL) was kept at 120 °C, with magnetic stirring (1200 r/min). Oxygen was flowed into the suspension at a rate of 20 mL/min. The liquid products were obtained by centrifugation, and then analyzed using a gas chromatograph (GC-1690, Hangzhou Jiedao Technology Instrument Co., Ltd) equipped with a flame ionization detector (FID) and an AT OV-1701 capillary column, to determine the conversion and selectivity. Gas chromatography-mass spectrometry (GC-MS; 450GC-320MS, Varian) was used to confirm the product compositions.

The catalysts were recovered by centrifugation, washed alternately with ethanol and water several times, and dried at 90 °C overnight. The recovered catalyst was used to investigate the recycling performance under the same reaction conditions.

3. Results and discussion

3.1. Catalyst characterization

The N_2 adsorption-desorption isotherms of Au/HAP, CuO/HAP, and Au/CuO-HAP are shown in Fig. 1(a). The relative pressure was set in the range 0.01–1.0. The surface areas of

Au/HAP, CuO-HAP, and Au/CuO-HAP were 53.8, 50.8, and 53.7 m^2/g, respectively. There were no significant differences among the specific surface areas, and sickle-shaped N_2 adsorption-desorption isotherms were observed for all three catalysts. Fig. 1(b) shows that the major peak for the three catalysts was located at 27 nm. However, after loading with Cu species, a shoulder peak appeared at about 39 nm for both CuO-HAP and Au/CuO-HAP, indicating that the Cu species altered the porous structure; these results are consistent with those in the literature [30].

Fig. 2 shows the TEM and HRTEM images of Au/HAP, CuO-HAP, and Au/CuO-HAP and their metal particle size distribution diagrams. Fig. 2(a) shows that the Au NPs are well dispersed on nanosized HAP, with an average diameter of 3.8 nm. The measured interplanar distances of 0.235 and 0.343 nm correspond to the spacing of the (111) plane of face-centered cubic Au NPs (PDF No. 04-0784) and the spacing of the (002) plane of HAP (PDF No. 09-0432), respectively (Fig. 2(d)). It is clear from Fig. 2(b) that a large number of small particles of average diameter (2.7 nm) are uniformly dispersed on the support; most of the particles are of size 2 to 3.5 nm. The lattice spacing of 0.232 nm corresponds to the (111) plane of monoclinic CuO NPs (PDF No. 48-1548; Fig. 2(e)). The TEM and HRTEM images of CuO-HAP confirm that a large number of CuO NPs were generated during support preparation, and that the support has the typical HAP structure, although some Cu^{2+} ions

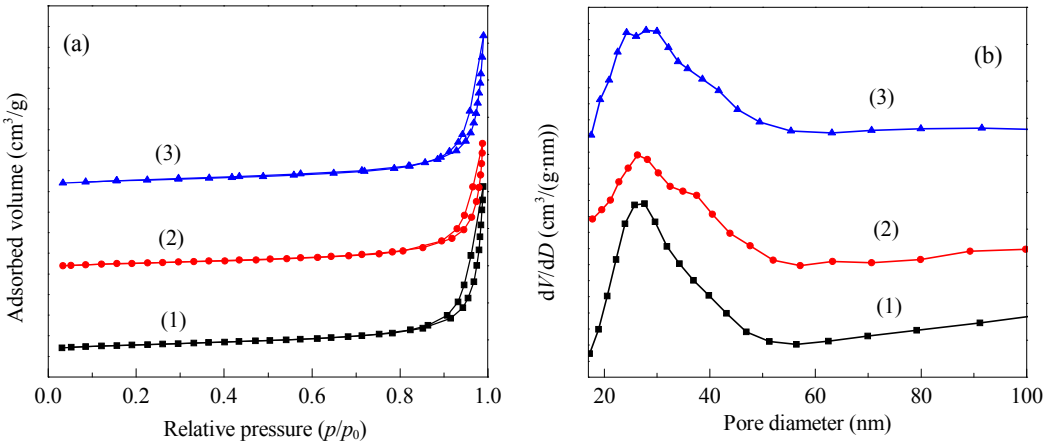

Fig. 1. N_2 adsorption-desorption isotherms (a) and BJH pore size distributions (b) of Au/HAP (1), CuO/HAP (2), and Au/CuO-HAP (3).

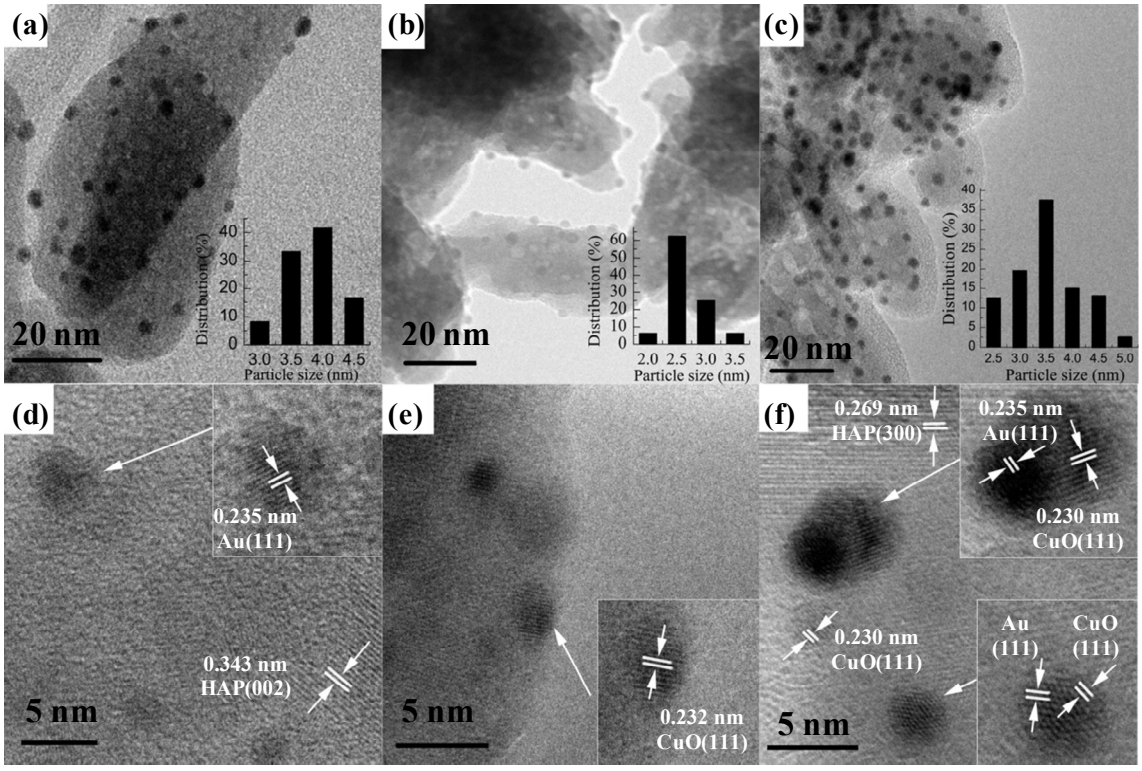

Fig. 2. TEM images and corresponding particle size distributions of Au/HAP (a), CuO-HAP (b), and Au/CuO-HAP (c); HRTEM images of Au/HAP (d), CuO-HAP (e), and Au/CuO-HAP (f).

might dope into the HAP network. When the solution of copper(II) chloride and phosphoric acid was added dropwise to the calcium hydroxide suspension at 80 °C (as described in the experimental section), copper hydroxide was more easily precipitated than copper phosphate, because the former is less soluble at pH = 9.0. As a result, large amounts of CuO NPs were generated when copper hydroxide decomposed at high temperature. Fig. 2(c) shows that Au and CuO NPs of average diameter (3.5 nm) are finely dispersed on the CuO-HAP support. Little NPs aggregation was observed, possibly because of the high surface area of the porous structure of CuO-HAP or the sinter-resistant properties of CuO. The HRTEM image of Au/CuO-HAP shows the presence of CuO NPs and bimetallic Au-CuO NPs. The interplanar distance of 0.269 nm corresponds to the (300) crystal plane of the HAP support (Fig. 2(f)).

XPS was used to determine the surface chemical states of Au and Cu in the samples. Fig. 3 shows the Au 4*f* and Cu 2$p_{3/2}$ XPS profiles of Au/HAP, Au/CuO-HAP, and CuO-HAP. The Au 4*f* spectra of Au/HAP and Au/CuO-HAP (Fig. 3(a)) show that the binding energies of Au in Au/HAP at 87.5 and 83.8 eV are attributable to Au 4$f_{5/2}$ and 4$f_{7/2}$, respectively, the Au 4$f_{5/2}$ and 4$f_{7/2}$ binding energies in Au/CuO-HAP shifted to 87.8 and 84.1 eV, respectively. The 0.3 eV positive shift for Au/CuO-HAP compared with Au/HAP was probably caused by interactions between Au NPs and CuO NPs. After four runs of benzyl alcohol oxidation, the Au chemical state of the used Au/CuO-HAP was almost unchanged. The asymmetric Cu 2$p_{3/2}$ peaks in the spectra of fresh Au/CuO-HAP and CuO-HAP can be fitted to two peaks, at 933.5 and 935.0 eV, which are attributed to the binding energies of Cu 2$p_{3/2}$ in CuO and copper phosphate, respectively [30,31]. The characteristic shake-up satellite peak at the higher binding energy of 944 eV for Cu^{2+} also indicates that the main components were Cu^{2+} species. The peak-fitting results indicate that the atomic ratio of Cu from CuO to Cu from copper phosphate in both CuO-HAP and Au/CuO-HAP was close to 4:1, i.e., in Au/CuO-HAP and CuO-HAP, Cu was mainly present in the CuO state, with a small amount of Cu doped into the HAP network; these results are consistent with the TEM images. However, in Fig. 3(b), the peak in the Cu 2$p_{3/2}$ spectrum of the used Au/CuO-HAP shifted from 933.6 to 933.0 eV, and was fitted to three peaks, at 935.0, 933.5, and 932.5 eV, which correspond to the binding energies of Cu 2$p_{3/2}$ in copper phosphate, CuO, and Cu_2O, respectively. The weakened shake-up satellite peak also indicates that the Cu^{2+} was partially reduced. Area integration showed that about 50% of surface Cu was transformed into Cu_2O in the used Au/CuO-HAP. It is easy to see that CuO was partially reduced to Cu_2O in the presence of benzyl alcohol under alkaline conditions; during this process, CuO could supply active oxygen for the reaction [28].

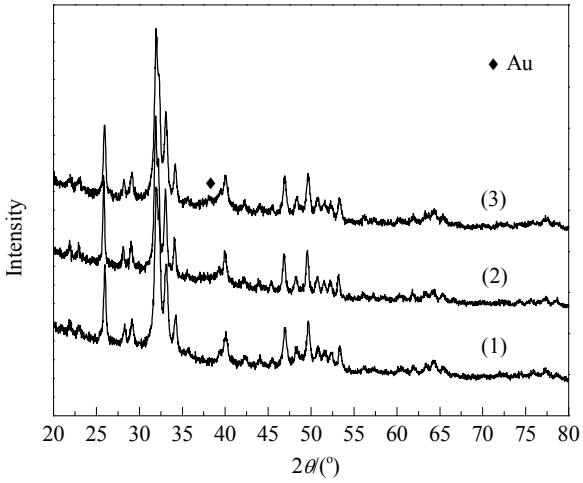

Fig. 4. XRD patterns of CuO-HAP (1), Au/HAP (2), and Au/CuO-HAP (3).

Fig. 4 shows the XRD patterns of CuO-HAP, Au/HAP, and Au/CuO-HAP. The major diffraction peaks for CuO-HAP, Au/HAP, and Au/CuO-HAP, at 2θ = 25.9°, 31.9°, 33.1°, and 34.1°, are almost identical, and in good agreement with the typical HAP structure (PDF No. 09-0432). These results show that the prepared CuO-HAP and HAP were stable during Au NPs loading, and the HAP structure was not changed by the small amount of Cu doping. Although the Au and Cu contents in Au/CuO-HAP were both 4%, only a weak and broad diffraction peak at 2θ = 38.2°, associated with the Au (111) plane, can be

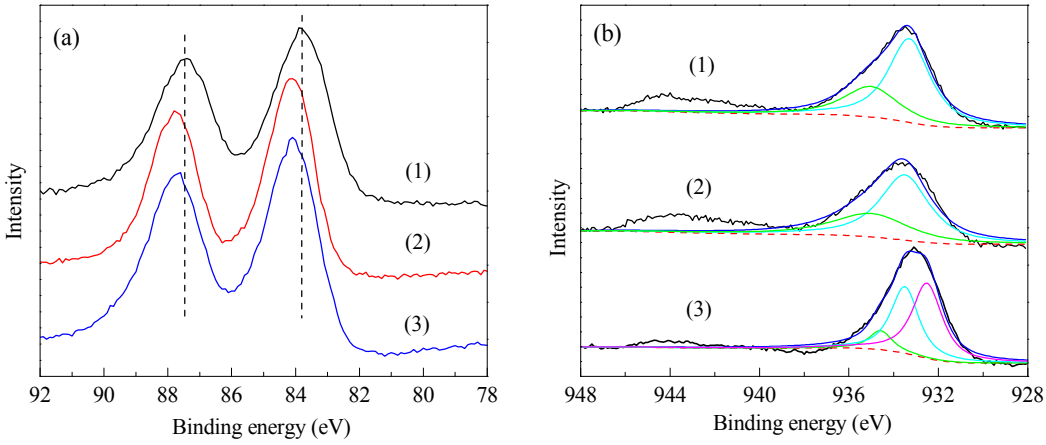

Fig. 3. (a) Au 4*f* XPS profiles of Au/HAP (1), fresh Au/CuO-HAP (2), and used Au/CuO-HAP (3), and (b) Cu 2$p_{3/2}$ XPS profiles of CuO-HAP (1), fresh Au/CuO-HAP (2), and used Au/CuO-HAP (3).

identified; this is attributed to the effect of the small finely dispersed Au and CuO NPs.

3.2. Catalytic performance in benzyl alcohol oxidation

In the aerobic oxidation of benzyl alcohol catalyzed by monometallic Au catalysts, by-products such as toluene, benzoic acid, and benzyl benzoate are easily formed [15,32]. Bimetallic Au catalysts have enhanced activity and selectivity in alcohol oxidation [18,27]. The catalytic performance of the Au/HAP, CuO-HAP, and Au/CuO-HAP catalysts in the aerobic oxidation of benzyl alcohol are summarized in Table 1. When CuO-HAP was used, only 4.5% of benzyl alcohol was converted to benzaldehyde after reaction for 1.5 h, indicating that this catalyst had low catalytic activity in this reaction. Under the same reaction conditions, Au/HAP exhibited higher catalytic activity, and 53.2% and 98.9% conversions of benzyl alcohol were achieved after 1 and 4 h, respectively. However, the selectivity for benzaldehyde decreased from 96.2% to 91.4%, and about 9% benzyl benzoate was generated as a by-product, because of over oxidation. Benzyl alcohol was quantitatively converted to benzaldehyde over Au-CuO/HAP after 1.5 h, and the selectivity for benzaldehyde remained greater than 98.4%, without over oxidation. The calculated turnover frequencies (TOFs) of Au/CuO-HAP and Au/HAP were 548 and 460 h^{-1}, respectively, indicating that Au/CuO-HAP had higher catalytic activity in the aerobic oxidation of benzyl alcohol. We suggest that the enhanced catalytic performance of Au/CuO-HAP in the aerobic oxidation of benzyl alcohol is the result of a synergistic effect between the supported Au and CuO NPs.

3.3. Scope of Au/CuO-HAP-catalyzed alcohol oxidation

The scope for the Au/CuO-HAP-catalyzed aerobic oxidation of alcohols was investigated. Table 2 lists the results for aerobic oxidation of various alcohols catalyzed by Au/CuO-HAP. The oxidation of benzyl alcohol and its derivatives with electron-donating groups to the corresponding aldehydes (entries 1–3) was easier than the oxidation of benzyl alcohol with an electron-withdrawing group (entry 4). Although the catalytic activity in the reaction with 2-furanmethanol was low, the selectivity for furfuraldehyde was greater than 97.5% (entry 5). Cinnamyl alcohol and diphenylmethanol were also quantitatively converted to their corresponding aldehyde and ketone with high TOF values (entries 6 and 7).

Table 1
Catalytic performance of Au/HAP, CuO-HAP, and Au/CuO-HAP in oxidation of benzyl alcohol.

Catalyst	Au [a] (%)	Cu [a] (%)	Size (nm)	Time (h)	Conversion [b] (%)	Benzaldehyde selectivity [b] (%)	TOF [c] (h^{-1})
CuO-HAP	—	3.9	2.7	1.0	1.5	0	—
				1.5	4.5	100	
Au/HAP	4.3	—	3.8	1.0	53.2	96.2	460
				1.5	75.7	93.1	
				4.0	98.9	91.4	
Au/CuO-HAP	4.7	3.7	3.5	1.0	95.9	98.6	548
				1.5	99.7	98.4	

Reaction conditions: 3 mmol benzyl alcohol, 1 mmol K_2CO_3, 50 mg catalyst, 10 mL *p*-xylene, 20 mL/min O_2, 120 °C.
[a] The contents of Au and Cu were measured by AAS. [b] Products conducted by GC-FID. [c] TOF value was calculated as: mol of benzyl alcohol converted at the first 15 min/(mol of total loading of Au × reaction time).

Table 2
Results for oxidation of various alcohols over Au-CuO/HAP in *p*-xylene.

Entry	Substrate	Conversion [a] (%)	Aldehyde/ketone selectivity [a] (%)	Time (h)	TOF [b] (h^{-1})
1	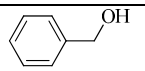	99.7	98.4	1.5	548
2	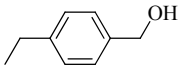	99.7	>99.9	3.5	414
3	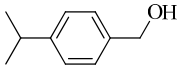	99.8	99.7	3.5	405
4 [c]	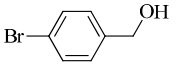	94.5	>99.9	7.0	119
5	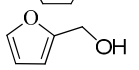	89.8	97.5	9.0	99
6	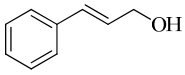	99.6	99.5	4.0	254
7	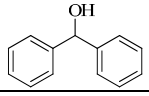	99.9	>99.9	1.5	536

Reaction conditions: 3 mmol alcohol, 1 mmol K_2CO_3, 50 mg Au/CuO-HAP catalyst, 10 mL *p*-xylene, 20 mL/min O_2, 120 °C.
[a] Products conducted by GC-FID. [b] TOF value was calculated as: mol of alcohol converted at the first 15 min/(mol of total loading of Au × reaction time). [c] 0.1 g Au/CuO-HAP catalyst.

3.4. Reusability of Au/CuO-HAP catalyst

Catalyst reusability is important in industry. As a result of aggregation, particle size enlargement, and support instability, the catalytic performance of heterogeneous Au catalysts in liquid-phase oxidation of alcohols deteriorate in recycling experiments [15,33,34]. The recycling performance of the Au/CuO-HAP catalyst in the oxidation of benzyl alcohol was investigated. Table 3 lists the benzyl alcohol conversion and selectivity for benzaldehyde over recycled Au/CuO-HAP at 120 °C after reaction for 1.5 h. Under the same aerobic conditions, the catalytic performance of Au/CuO-HAP from the second to the fourth runs was almost unchanged, and the benzyl alcohol conversion and selectivity for benzaldehyde was above 95% and 99%, respectively, i.e., similar to those with the fresh catalyst (the first run). The TEM image of Au/CuO-HAP after the fourth run (Fig. 5) shows that the Au particle size had not noticeably altered, most of the Au NPs were of size 2.5 to 4.5 nm, and no aggregation was observed. The XPS results show that the chemical state of Au did not change and about 50% of surface Cu was transformed into Cu_2O in the catalyst after the fourth run (see Fig. 3). The change in the surface Cu structure did not significantly affect the catalytic activity of the reused Au/CuO-HAP, indicating that the activity was dominated by Au, with a minor contribution from CuO. CuO NPs on the HAP sur-

Table 3
Au/CuO-HAP recycling experiments.

Run number	Conversion of benzyl alcohol (%)	Benzaldehyde selectivity (%)
1st	99.7	98.4
2nd	95.8	99.2
3rd	97.2	99.5
4th	96.3	99.2

Reaction conditions: 3 mmol benzyl alcohol, 1 mmol K_2CO_3, 50 mg Au/CuO-HAP catalyst, 10 mL *p*-xylene, 20 mL/min O_2, 120 °C, 1.5 h.

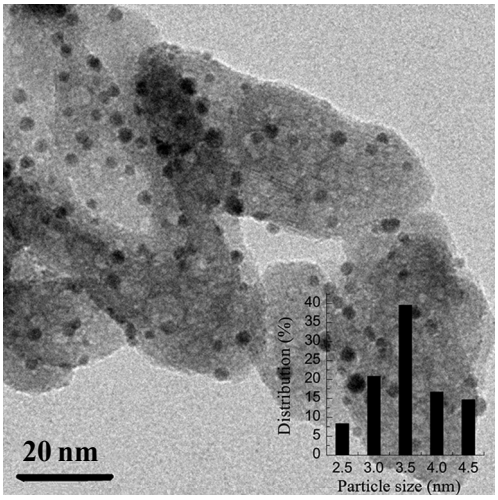

Fig. 5. TEM image and particle size distribution of Au/CuO-HAP catalyst after the fourth run.

face may act as anchors, protecting the Au NPs from aggregation.

4. Conclusions

A bimetallic catalyst, i.e., Au/CuO-HAP, with an average particle diameter of 3.5 nm was prepared by a simple method and used in the liquid-phase aerobic oxidation of alcohols. The catalytic performance of Au/CuO-HAP in the aerobic oxidation of benzyl alcohol was better than that of monometallic Au/HAP and CuO-HAP catalysts, because of the bimetallic synergistic effect. Various aromatic alcohols were converted to their corresponding aldehydes or ketones over Au/CuO-HAP, with high catalytic activity and excellent selectivity. The Au NPs were anchored on the support by CuO NPs, and had excellent size stability. The prepared Au/CuO-HAP catalyst can be reused at least four times without loss of its activity.

References

[1] Sheldon R A, Kochi J K. Metal-Catalyzed Oxidations of Organic Compounds. New York: Academic Press, 1981
[2] Cossio F P, Lopez M C, Palomo C. *Tetrahedron*, 1987, 43: 3963
[3] Lee D G, Spitzer U A. *J Org Chem*, 1970, 35: 3589
[4] Menger. F M, Lee C. *J Org Chem*, 1979, 44: 3446
[5] Jefford C W, Wang Y. *J Chem Soc, Chem Commun*, 1988: 634
[6] Weerasiri K C, Gorden A E V. *Tetrahedron*, 2014, 70: 7962
[7] Sato K, Aoki M, Takagi J, Noyori R. *J Am Chem Soc*, 1997, 119: 12386
[8] Dhakshinamoorthy A, Alvaro M, Garcia H. *ACS Catal*, 2011, 1: 48
[9] Dun R R, Wang X G, Tan M W, Huang Z, Huang X M, Ding W Z, Lu X G. *ACS Catal*, 2013, 3: 3063
[10] Wang L, Meng X J, Xiao F S. *Chin J Catal*, 2010, 31: 943
[11] Hong Y J, Yan X Q, Liao X F, Li R H, Xu S D, Xiao L P, Fan J. *Chem Commun*, 2014, 50: 9679
[12] Gopiraman M, Ganesh Babu S, Khatri Z, Kai W, Kim Y A, Endo M, Karvembu R, Kim I S. *J Phys Chem C*, 2013, 117: 23582
[13] Haruta M, Yamada N, Kobayashi T, lijima S. *J Catal*, 1989, 115: 301
[14] Haruta M, Tsubota S, Kobayashi T, Kageyama H, Genet M J, Delmon B. *J Catal*, 1993, 144: 175
[15] Wang Z, Xu C L, Wang H F. *Catal Lett*, 2014, 144: 1919
[16] Wang L, Zhang W, Su D S, Meng X J, Xiao F S. *Chem Commun*, 2012, 48: 5476
[17] Kesavan L, Tiruvalam R, Ab Rahim M H, bin Saiman M I, Enache D I, Jenkins R L, Dimitratos N, Lopez-Sanchez J A, Taylor S H, Knight D W, Kiely C J, Hutchings G J. *Science*, 2011, 331: 195
[18] Enache D I, Edwards J K, Landon P, Solsona-Espriu B, Carley A F,

Graphical Abstract

Chin. J. Catal., 2015, 36: 1358–1364 doi: 10.1016/S1872-2067(15)60854-3

Bimetallic synergistic Au/CuO-hydroxyapatite catalyst for aerobic oxidation of alcohols

Tao Tian, Ying Liu, Xungao Zhang*
Wuhan University

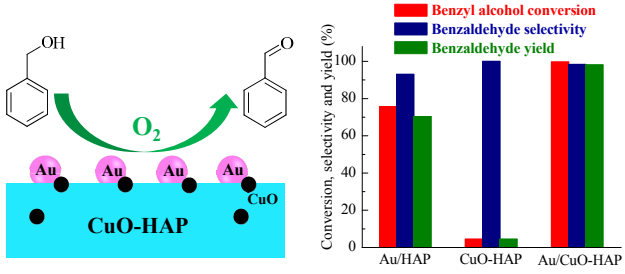

The catalytic activity and benzaldehyde selectivity of bimetallic Au/CuO-HAP in the oxidation of benzyl alcohol were better than those of monometallic Au/HAP and CuO/HAP catalysts.

Herzing A A, Watanabe M, Kiely C J, Knight D W, Hutchings G J. *Science*, 2006, 311: 362

[19] Yang X, Chen D, Liao S J, Song H Y, Li Y W, Fu Z Y, Su Y L. *J Catal*, 2012, 291: 36

[20] Lopez-Sanchez J A, Dimitratos N, Glanville N, Kesavan L, Hammond C, Edwards J K, Carley A F, Kiely C J, Hutchings G J. *Appl Catal A*, 2011, 391: 400

[21] Zhao J G, Cheng X G, Wang L, Ren R F, Zeng J J, Yang H H, Shen B X. *Catal Lett*, 2014, 144: 2191

[22] Zhang H Y, Dai B, Wang X G, Li W, Han Y, Gu J J, Zhang J L. *Green Chem*, 2013, 15: 829

[23] Potemkin D I, Semitut E Yu, Shubin Yu V, Plyusnin P E, Snytnikov P V, Makotchenko E V, Osadchii D Y, Svintsiskiy D A, Venyaminov S A, Korenev S V, Sobyanin V A. *Catal Today*, 2014, 235: 103

[24] Neaţu Ş, Maciá-Agulló J A, Concepción P, Garcia H. *J Am Chem Soc*, 2014, 136: 15969

[25] Yuan X, Zheng J W, Zhang Q, Li S R, Yang Y H, Gong J L. *AIChE J*, 2014, 60: 3300

[26] Jia Q Q, Zhao D F, Tang B, Zhao N, Li H D, Sang Y H, Bao N, Zhang X M, Xu X H, Liu H. *J Mater Chem A*, 2014, 2: 16292

[27] Li W J, Wang A Q, Liu X Y, Zhang T. *Appl Catal A*, 2012, 433-434: 146

[28] Wang H, Fan W B, He Y, Wang J G, Kondo J N, Tatsumi T. *J Catal*, 2013, 299: 10

[29] Zanella R, Giorgio S, Shin C H, Henry C R, Louis C. *J Catal*, 2004, 222: 357

[30] Wen C, Cui Y Y, Chen X, Zong B N, Dai W L. *Appl Catal B*, 2015, 162: 483

[31] Moulder J F, Stickle W F, Sobol P E, Bomben K D. Handbook of X-ray Photoelectron Spectroscopy. Minnesota: Physical Electronics, 1995

[32] Wang L C, He L, Liu Q, Liu Y M, Chen M, Cao Y, He H Y, Fan K N. *Appl Catal A*, 2008, 344: 150

[33] Li X, Zheng J M, Yang X L, Dai W L, Fan K N. *Chin J Catal*, 2013, 34: 1013

[34] Hallett-Tapley G L, Silvero M J, Bueno-Alejo C J, González-Béjar M, McTiernan C D, Grenier M, Netto-Ferreira J C, Scaiano J C. *J Phys Chem C*, 2013, 117: 12279